NLO QCD corrections to pseudoscalar quarkonium production with two heavy flavors in photon-photon collision

Hao Yang,[1,†] Zi-Qiang Chen,[2,‡] and Cong-Feng Qiao[1,3,*]

[1]*School of Physics, University of Chinese Academy of Sciences, Yuquan Road 19A, Beijing 100049, China*
[2]*School of Physics and Materials Science, Guangzhou University, Guangzhou 51006, China*
[3]*CAS Key Laboratory of Vacuum Physics, Beijing 100049, China*

(Received 29 March 2022; accepted 2 May 2022; published 16 May 2022)

We calculate the next-to-leading order (NLO) QCD corrections to $\gamma+\gamma\to\eta_c+c+\bar{c}$, $\gamma+\gamma\to\eta_b+b+\bar{b}$, and $\gamma+\gamma\to B_c+b+\bar{c}$ processes in the framework of nonrelativistic QCD factorization formalism. The cross sections at the SuperKEKB electron-positron collider, as well as the future collider like the Circular Electron Positron Collider, are evaluated. Numerical results indicate that the NLO corrections are significant, and the uncertainties in theoretical predictions with NLO corrections are reduced as expected. Due to the high luminosity of the SuperKEKB collider, the $\eta_c+c+\bar{c}$ production is hopefully observable in the near future.

DOI: 10.1103/PhysRevD.105.094014

I. INTRODUCTION

Heavy quarkonium plays an important role in high energy collider physics, as it presents an ideal laboratory for studying the perturbative and nonperturbative properties of quantum chromodynamics (QCD) within a controlled environment. The nonelativistic QCD (NRQCD) factorization formalism [1], which was developed by Bodwin, Braaten, and Lepage, provides a systematic framework for the theoretical study of quarkonium production and decay. According to the NRQCD factorization formalism, quarkonium production rates can be written as a sum of products of short distance coefficients and the long distance matrix elements (LDMEs). The short distance coefficients can be calculated as a perturbation series in the strong-coupling constant α_s, and the LDMEs can be expanded in powers of the relative velocity v of the heavy quarks in the bound state. In this way, the theoretical prediction takes the form of a double expansion in α_s and v. Although the quarkonium production has been extensively investigated at various colliders, the existing researches are still not sufficient to clarify the underlying production mechanisms [2–5].

Quarkonium production in association with two heavy quarks via the massless vector boson fusion, i.e., $\gamma(g)+\gamma(g)\to\mathcal{Q}[Q_1\bar{Q}_2]+Q_2+\bar{Q}_1$, process (with Q_i representing the c or b quark) is an interesting topic to study. Experimentally, the techniques to tag heavy quarks are now routinely used with high efficiencies, hence the observation of these associated production processes is hopefully possible. On the other hand, as has been indicated by previous studies [6–15], these processes are the dominant color-singlet channels for corresponding single quarkonium inclusive production, and therefore be crucial for pinning down the contributions from color-singlet model. The color-octet channels for these processes are estimated to be suppressed by the color-octet LDMEs about two magnitudes. For B_c meson production, a similar mechanism is more important, as quark flavor conservation requires that the B_c meson should be produced in accompaniment with an additional $b\bar{c}$ pair. Despite the admitted importance, these processes are not fully investigated due to the high technical difficulty. At present, the only full next-to-leading order (NLO) study is in Ref. [15], where the NLO QCD corrections to the $\gamma+\gamma\to J/\psi+c+\bar{c}$ process is calculated. As a further step, in this work, we calculate the NLO QCD corrections to the $\gamma+\gamma\to\eta_c+c+\bar{c}$, $\gamma+\gamma\to\eta_b+b+\bar{b}$ and $\gamma+\gamma\to B_c+b+\bar{c}$ processes.

The rest of the paper is organized as follows. In Sec. II, we present the primary formulas employed in the calculation. In Sec. III, we elucidate some technical details for the analytical calculation. In Sec. IV, the numerical evaluation for concerned processes is performed. The last section is reserved for summary and conclusions.

*Corresponding author.
qiaocf@ucas.ac.cn
†yanghao174@mails.ucas.ac.cn
‡chenziqiang13@mails.ucas.ac.cn

II. FORMULATION

The photon-photon scattering can be achieved at e^+e^- collider like SuperKEKB, where the initial photons are generated by bremsstrahlung effect. The energy spectrum of bremsstrahlung photon is well formulated by Weizsacker-Williams approximation (WWA) [16]:

$$f_\gamma(x) = \frac{\alpha}{2\pi}\left(\frac{1+(1-x)^2}{x}\log\left(\frac{Q^2_{\max}}{Q^2_{\min}}\right) + 2m_e^2 x\left(\frac{1}{Q^2_{\max}} - \frac{1}{Q^2_{\min}}\right)\right), \tag{1}$$

where $Q^2_{\min} = m_e^2 x^2/(1-x)$, $Q^2_{\max} = (\theta_c\sqrt{s}/2)^2(1-x) + Q^2_{\min}$, m_e is the electron mass, $x = E_\gamma/E_e$ is the energy fraction of photon, $\sqrt{s}$ is the collision energy of the e^+e^- collider, $\theta_c = 32$ mrad [6] is the maximum scattering angle of the electron or positron.

In future e^+e^- collider like the Circular Electron Positron Collider (CEPC), high energy photon can be achieved through the Compton backscattering of laser light off an electron or positron beam, namely the laser backscattering (LBS) effect. The LBS photons mostly carry a large energy fraction of the incident electron or positron beam and, at the same time, can achieve high luminosity. The energy spectrum of LBS photon is [17]

$$f_\gamma(x) = \frac{1}{N}\left(1 - x + \frac{1}{1-x} - 4r(1-r)\right), \tag{2}$$

where $r = \frac{x}{x_m(1-x)}$ and N is the normalization factor:

$$N = \left(1 - \frac{4}{x_m} - \frac{8}{x_m^2}\right)\log(1+x_m) + \frac{1}{2} + \frac{8}{x_m} - \frac{1}{2(1+x_m)^2}. \tag{3}$$

Here $x_m \approx 4.83$ [18], and the maximum energy fraction of the LBS photon is restricted by $0 \le x \le \frac{x_m}{1+x_m} \approx 0.83$.

The total cross section can be obtained by convoluting the $\gamma+\gamma \to \mathcal{Q}[Q_1\bar{Q}_2] + Q_2 + \bar{Q}_1$ cross section with the photon distribution functions:

$$d\sigma = \int dx_1 dx_2 f_\gamma(x_1) f_\gamma(x_2) d\hat{\sigma}(\gamma+\gamma \to \mathcal{Q}[Q_1\bar{Q}_2] + Q_2 + \bar{Q}_1), \tag{4}$$

where $\mathcal{Q} = \eta_c$, η_b, or B_c, and Q_i denotes charm or bottom quark accordingly. The $d\hat{\sigma}$ is calculated perturbatively up to the NLO level,

$$d\hat{\sigma}(\gamma+\gamma \to \mathcal{Q}[Q_1\bar{Q}_2] + Q_2 + \bar{Q}_1) = d\hat{\sigma}_{\text{born}} + d\hat{\sigma}_{\text{virtual}} + d\hat{\sigma}_{\text{real}} + \mathcal{O}(\alpha^2\alpha_s^4). \tag{5}$$

The Born level cross section, the virtual correction, and the real correction take the following forms:

$$\begin{aligned} d\hat{\sigma}_{\text{born}} &= \frac{1}{2\hat{s}}\overline{\sum}|\mathcal{M}_{\text{tree}}|^2 d\text{PS}_3, \\ d\hat{\sigma}_{\text{virtual}} &= \frac{1}{2\hat{s}}\overline{\sum}2\text{Re}(\mathcal{M}^*_{\text{tree}}\mathcal{M}_{\text{one-loop}})d\text{PS}_3, \\ d\hat{\sigma}_{\text{real}} &= \frac{1}{2\hat{s}}\overline{\sum}|\mathcal{M}_{\text{real}}|^2 d\text{PS}_4, \end{aligned} \tag{6}$$

where $\hat{s}$ is the center-of-mass energy square for the two photons, $\overline{\sum}$ means sum (average) over the polarizations and colors of final (initial) state particles, $d\text{PS}_3$ ($d\text{PS}_4$) denotes final state three- (four-)body phase space.

The computation of $d\hat{\sigma}$ can be carried out by using the covariant projection method [19]. At the leading order of relative velocity expansion, the standard spin and color projection operator can be simplified to

$$\Pi = \frac{1}{2\sqrt{m_\mathcal{Q}}}\gamma^5(\not{p}_\mathcal{Q} + m_\mathcal{Q}) \otimes \left(\frac{\mathbf{1_c}}{\sqrt{N_c}}\right), \tag{7}$$

where $p_\mathcal{Q}$ and $m_\mathcal{Q}$ are the momentum and mass of the pseudoscalar quarkonium $\mathcal{Q}$, respectively, $\mathbf{1_c}$ represents the unit color matrix, and $N_c = 3$ is the number of colors in QCD.

III. ANALYTICAL CALCULATION

At LO, there are 20 Feynman diagrams contributing to the $\gamma+\gamma \to \mathcal{Q}[Q_1\bar{Q}_2] + Q_2 + \bar{Q}_1$ process. Half of them are shown in Fig. 1, and the rest can be generated by exchanging the initial two photons. The typical Feynman diagrams in virtual correction are shown in Fig. 2. Therein, loops N1–N5 and loop N11 arise from the corrections to LO Feynman diagrams, and the rest are new topologies appearing at NLO. We note that, according to the charge-parity conservation, the contributions of type loop N6 diagrams are vanished, which is verified by our explicit calculation. And obviously, loops N6–N10 will not appear in the B_c production case.

In the computation of virtual corrections, the conventional dimensional regularization with $D = 4-2\epsilon$ is employed to regularize the ultraviolet (UV) divergences, while the infrared (IR) divergences are regularized by introducing an infinitesimal gluon mass λ. The gluon mass regularization scheme breaks gauge invariance and is applicable only if the triple-gluon vertex does not play a role in the process, fortunately we should not worry about this due to the IR divergent diagrams for the processes considered here are all QED-like. As a result, the UV and IR singularities appear as $1/\epsilon$ and $\ln(\lambda^2)$ terms, respectively.

In renormalized perturbation theory, the UV singularities are canceled by corresponding counterterm diagrams,

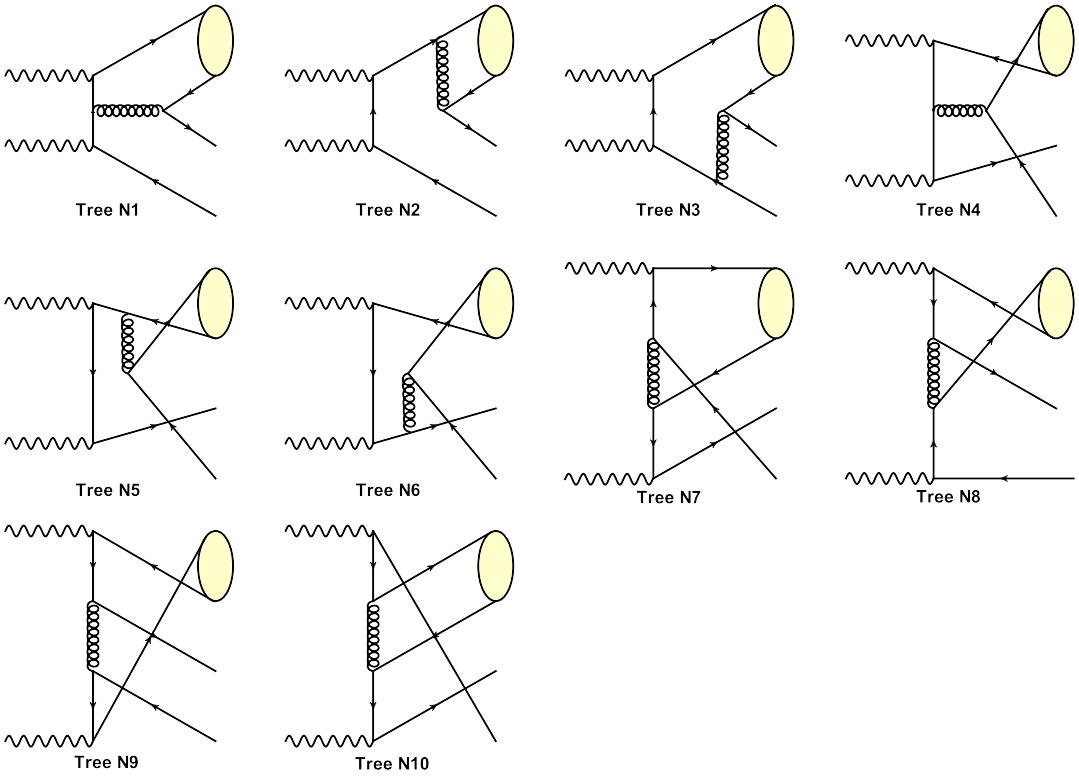

FIG. 1. Typical LO Feynman diagrams for $\gamma + \gamma \to \mathcal{Q}[Q_1\bar{Q}_2] + Q_2 + \bar{Q}_1$ process.

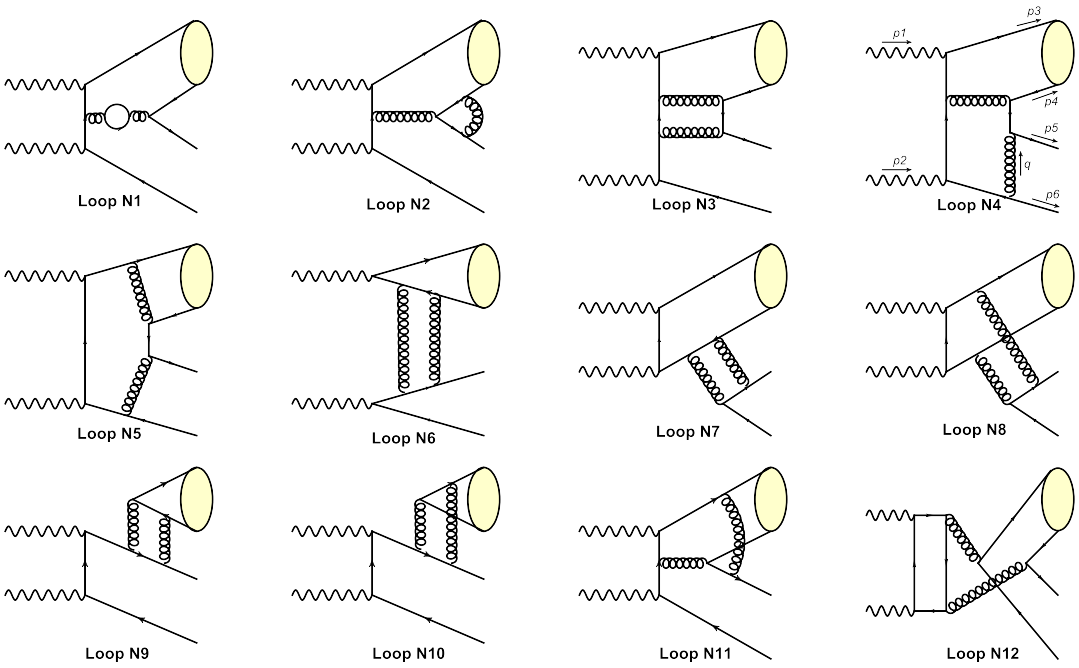

FIG. 2. Typical Feynman diagrams in virtual corrections.

hence the final virtual corrections are UV finite. Here, the relevant renormalization constants include Z_2, Z_3, Z_m, and Z_g, which correspond to the heavy quark field, gluon field, heavy quark mass, and strong coupling constant, respectively. Among them, Z_2 and Z_m are defined in the on-mass-shell (OS) scheme, while others are defined in the modified minimal-subtraction ($\overline{\text{MS}}$) scheme. The counterterms are

$$\delta Z_2^{\rm OS} = -C_F \frac{\alpha_s}{4\pi}\left[2\ln\frac{\lambda^2}{m^2} + \frac{1}{\epsilon_{\rm UV}} - \gamma_E + \ln\frac{4\pi\mu^2}{m^2} + 4\right],$$
$$\delta Z_m^{\rm OS} = -3C_F \frac{\alpha_s}{4\pi}\left[\frac{1}{\epsilon_{\rm UV}} - \gamma_E + \ln\frac{4\pi\mu^2}{m^2} + \frac{4}{3}\right],$$
$$\delta Z_3^{\overline{\rm MS}} = (\beta_0 - 2C_A)\frac{\alpha_s}{4\pi}\left[\frac{1}{\epsilon_{\rm UV}} - \gamma_E + \ln(4\pi)\right],$$
$$\delta Z_g^{\overline{\rm MS}} = -\frac{\beta_0}{2}\frac{\alpha_s}{4\pi}\left[\frac{1}{\epsilon_{\rm UV}} - \gamma_E + \ln(4\pi)\right], \tag{8}$$

where γ_E is the Euler's constant, μ is the renormalization scale, m stands for m_c or m_b, $\beta_0 = \frac{11}{3}C_A - \frac{4}{3}T_F n_f$ is the one-loop coefficient of the QCD β function, n_f denotes the active quark flavor numbers, and $C_A = 3, C_F = \frac{4}{3}$, and $T_F = \frac{1}{2}$ are QCD color factors. Note that, since there is no gluon external leg, the final result is independent of δZ_3.

The IR singularities in virtual corrections can be isolated by using the method proposed in [20]. Considering the scalar five-point integral of Fig. 2, loop N4, the IR singularities originate from $q \to 0$ region. By performing power counting analysis, we have

$$E_0 = \frac{1}{i\pi^2}\int \frac{d^4q}{(2\pi)^4}\frac{1}{q^2-\lambda^2}\frac{1}{(q-p_5)^2-m^2}\frac{1}{(q-p_4-p_5)^2-\lambda^2}\frac{1}{(q+p_6-p_2)^2-m^2}\frac{1}{(q+p_6)^2-m^2}$$
$$\underset{\sim}{\rm soft}\frac{1}{(p_4+p_5)^2}\frac{1}{(p_6-p_2)^2-m^2}C_0(p_6^2,(p_5+p_6)^2,p_5^2,\lambda^2,m^2,m^2)$$
$$\underset{\sim}{\rm soft}\frac{1}{s_{45}(t_{26}-m^2)}\frac{\ln(\lambda^2)}{\sqrt{s_{56}(s_{56}-4m^2)}}\left(\ln\frac{\sqrt{s_{56}}-\sqrt{s_{56}-4m^2}}{\sqrt{s_{56}}+\sqrt{s_{56}-4m^2}}+i\pi\right), \tag{9}$$

where $s_{45}=(p_4+p_5)^2$, $s_{56}=(p_5+p_6)^2$, $t_{26}=(p_2-p_6)^2$.

The Coulomb singularities, which appear when a potential gluon is exchanged between the constituent quarks of a quarkonium, are also regularized by the infinitesimal gluon mass λ. We obtain

$$2{\rm Re}(\mathcal{M}^*_{\rm tree}\mathcal{M}_{\rm oneloop})\ \underset{\sim}{\rm Coulomb}\ |\mathcal{M}_{\rm tree}|^2\frac{2\alpha_s C_F m}{\lambda}, \tag{10}$$

which can be absorbed into the wave function of quarkonium. Note, for B_c production, the m in Eq. (10) should be replaced by $\frac{2m_b m_c}{m_b+m_c}$.

Typical Feynman diagrams in real corrections are shown in Fig. 3. The IR divergences here are also regularized by infinitesimal gluon mass. To isolate the IR singularities, the subtraction method that was formulated in Ref. [21] is employed. As a result, the contribution of real corrections can be separated into two parts:

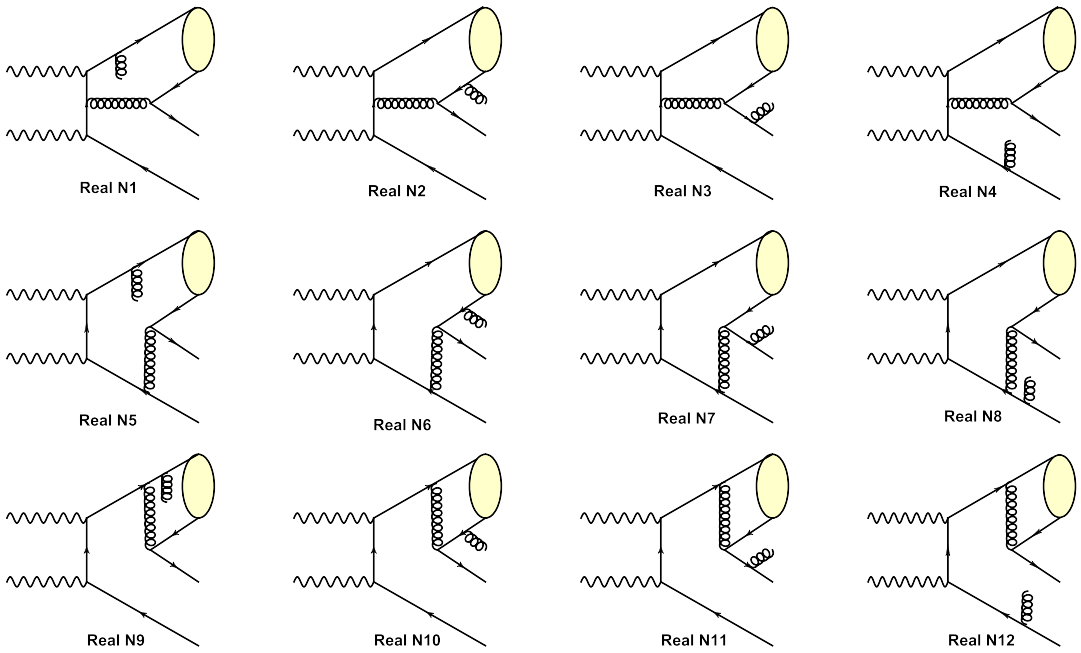

FIG. 3. Typical Feynman diagrams in real corrections.

$$\hat{\sigma}_{\rm real} = \hat{\sigma}^A_{\rm real} + \hat{\sigma}^B_{\rm real}, \tag{11}$$

with

$$\hat{\sigma}^A_{\rm real} = \frac{1}{2\hat{s}} \int d{\rm PS}_4 \left(\overline{\sum} |\mathcal{M}_{\rm real}|^2 - |\mathcal{M}_{\rm sub}|^2 \right), \tag{12}$$

$$\hat{\sigma}^B_{\rm real} = \frac{1}{2\hat{s}} \int d{\rm PS}_4 |\mathcal{M}_{\rm sub}|^2 = \frac{1}{2\hat{s}} \int d{\rm PS}_3 \int [dp_g] |\mathcal{M}_{\rm sub}|^2. \tag{13}$$

Here $[dp_g]$ denotes the phase space of the additional emitted gluon, and $|\mathcal{M}_{\rm sub}|^2$ is an auxiliary subtraction function that holds the same asymptotic behavior as $\overline{\sum}|\mathcal{M}_{\rm real}|^2$ in the soft limits. Hence the difference $(\overline{\sum}|\mathcal{M}_{\rm real}|^2 - |\mathcal{M}_{\rm sub}|^2)$ is nonsingular at each point of phase space, and the integral can be evaluated with $\lambda = 0$ everywhere. With an appropriate construction of $|\mathcal{M}_{\rm sub}|^2$ [21], the integral $\int [dp_g] |\mathcal{M}_{\rm sub}|^2$ can be carried out analytically. After adding $2{\rm Re}(\mathcal{M}^*_{\rm tree}\mathcal{M}_{\rm oneloop})$ and $\int [dp_g] |\mathcal{M}_{\rm sub}|^2$, the IR singularities, i.e., $\ln(\lambda^2)$ terms, cancel with each other as expected.

IV. NUMERICAL RESULTS

In the numerical calculation, the input parameters are taken as

$$\alpha = 1/137.065, \quad m_e = 0.511 \text{ MeV}, \quad m_c = 1.5 \text{ GeV}, \quad m_b = 4.8 \text{ GeV},$$
$$|R^{\rm LO}_{\eta_c}(0)|^2 = 0.528 \text{ GeV}^3, \quad |R^{\rm NLO}_{\eta_c}(0)|^2 = 0.907 \text{ GeV}^3,$$
$$|R^{\rm LO}_{\eta_b}(0)|^2 = 5.22 \text{ GeV}^3, \quad |R^{\rm NLO}_{\eta_b}(0)|^2 = 7.48 \text{ GeV}^3, \quad |R_{B_c}(0)|^2 = 1.642 \text{ GeV}^3.$$

Here, the B_c wave function at the origin is estimated by using the Buchmueller-Tye potential [22]. According to the heavy quark spin symmetry of NRQCD at the leading order in relative velocity expansion [1], here we take $R_{\eta_c}(0) = R_{J/\psi}(0)$ and $R_{\eta_b}(0) = R_\Upsilon(0)$. The J/ψ and Υ radial wave functions at the origin are extracted from their leptonic widths.

$$\Gamma(\mathcal{Q} \to e^+e^-) = \frac{\alpha^2 e_Q^2}{m_Q^2} |R_\mathcal{Q}(0)|^2 \left(1 - 4C_F \frac{\alpha_s(\mu_0)}{\pi}\right), \qquad e_Q = \begin{cases} \frac{2}{3}, & \text{if } \mathcal{Q} = J/\psi \\ \frac{1}{3}, & \text{if } \mathcal{Q} = \Upsilon \end{cases}, \tag{14}$$

with $\mu_0 = 2m_Q$, $\Gamma(J/\psi \to e^+e^-) = 5.55$ keV, and $\Gamma(\Upsilon \to e^+e^-) = 1.34$ keV [23]. Note that the LO and NLO extractions are employed in the LO and NLO calculations, respectively.

In the NLO calculation, the two-loop formula,

$$\frac{\alpha_s(\mu)}{4\pi} = \frac{1}{\beta_0 L} - \frac{\beta_1 \ln L}{\beta_0^3 L^2}, \tag{15}$$

for the running coupling constant is employed, in which $L = \ln(\mu^2/\Lambda^2_{\rm QCD})$, $\beta_0 = \frac{11}{3}C_A - \frac{4}{3}T_F n_f$, $\beta_1 = \frac{34}{3}C_A^2 - 4C_F T_F n_f - \frac{20}{3}C_A T_F n_f$, with $n_f = 4$, $\Lambda_{\rm QCD} = 297$ MeV for η_c production, and $n_f = 5$, $\Lambda_{\rm QCD} = 214$ MeV for η_b and B_c production. For the LO calculation, the one-loop formula for the running coupling constant is used. We note that, for the computation of the LO contribution in the NLO cross section, the two-loop formula for the running coupling constant is employed. To estimate the effects of α_s and LDMEs settings on total cross section, different schemes adopted by previous researches [5,24–28] are compared, see Table I.

We investigate the production of $\eta_c + c + \bar{c}$ with WWA photons as the initial state at the SuperKEKB collider, where the beam energies of the positron and electron are 4 and 7 GeV respectively, yielding a center-of-mass energy of 10.6 GeV. In order to estimate the theoretical uncertainties induced by renormalization scale and charm quark mass, we set $\mu = r\sqrt{4m_c^2 + p_t^2}$ with $r = \{0.5, 1, 2\}$,

TABLE I. The LO (in brackets) and NLO total cross sections for $\eta_c + c + \bar{c}$ production via photon-photon fusion at the SuperKEKB collider using different schemes of α_s and LDMEs settings: I. The two-loop formula of the running coupling for the LO and NLO cross section with fixed LDMEs [24,25]. II. The one-loop formula of the running coupling for the LO cross section and the two-loop formula of the running coupling for the NLO cross section with LDMEs fixed [5,26]. III. The one-loop formula of the running coupling and the LO extraction of LDMEs for the LO cross section, the two-loop formula of the running coupling and the NLO extraction of LDMEs for the NLO cross section [27,28]. Here $m_c = 1.5$ GeV, $\mu = \sqrt{4m_c^2 + p_t^2}$, the transverse momentum cut 0.2 GeV $\le p_t \le$ 4.0 GeV is imposed to η_c meson, and the NLO extraction of LDMEs is employed for fixed LDMEs.

Scheme	I	II	III
σ (fb)	0.364(0.169)	0.364(0.293)	0.364(0.171)

TABLE II. The LO and NLO total cross sections for $\eta_c + c + \bar{c}$ production via photon-photon fusion at the SuperKEKB collider. Here $m_c = 1.5$ GeV and $\mu = r\sqrt{4m_c^2 + p_t^2}$ with $r = \{0.5, 1, 2\}$. The transverse momentum cut $0.2\ \text{GeV} \le p_t \le 4.0\ \text{GeV}$ is imposed to the η_c meson.

r	0.5	1	2
σ_{LO} (fb)	0.340	0.171	0.102
σ_{NLO} (fb)	0.622	0.364	0.244

TABLE III. The LO and NLO total cross sections for $\eta_c + c + \bar{c}$ production via photon-photon fusion at the SuperKEKB collider. Here $m_c = \{1.4, 1.5, 1.6\}$ GeV and $\mu = \sqrt{4m_c^2 + p_t^2}$. The transverse momentum cut $0.2\ \text{GeV} \le p_t \le 4.0\ \text{GeV}$ is imposed to the η_c meson.

m_c (GeV)	1.4	1.5	1.6
σ_{LO} (fb)	0.393	0.171	0.074
σ_{NLO} (fb)	0.813	0.364	0.156

$m_c = \{1.4, 1.5, 1.6\}$ GeV, and p_t is the transverse momentum of η_c. The corresponding results are shown in Tables II and III, respectively. It can be seen that the NLO corrections are significant, and the total cross sections are enhanced by a factor (defined as the K factor) of about 2.1. To measure the dependency of the cross section on renormalization scale and charm quark mass, we define $R_\mu = \frac{\sigma|_{r=0.5} - \sigma|_{r=2}}{\sigma|_{r=1}}$ and $R_m = \frac{\sigma|_{m_c=1.4} - \sigma|_{m_c=1.6}}{\sigma|_{m_c=1.5}}$. Then we have $R_\mu^{\text{LO}} = 1.39$, $R_\mu^{\text{NLO}} = 1.03$, $R_m^{\text{LO}} = 1.86$, and $R_m^{\text{NLO}} = 1.80$, which indicates that the theoretical uncertainties are slightly reduced by NLO corrections.

In the coming year, the instantaneous luminosity of the SuperKEKB collider may reach $8 \times 10^{35}\ \text{cm}^{-2}\,\text{s}^{-1}$ [29]. Then the yearly produced $\eta_c + c + \bar{c}$ events is estimated to be $(3.93 \sim 20.5) \times 10^3$. In experiment, η_c can be reconstructed through its $K\bar{K}\pi$ decay channel with the branching ratio $\text{Br}(\eta_c \to K\bar{K}\pi) = 7.3\%$ [23], and the tagging efficiency of charm quark is about 41% [30]. Therefore we expect to obtain $48 \sim 251$ $\eta_c + c + \bar{c}$ events per year, this will provide a test for the challenge [31] when making NRQCD prediction in the quarkonium production with low p_t, e.g., $\frac{p_t}{2m_Q} \le 3$, the NRQCD factorization may be violated by power corrections of order m_Q^4/p_t^4 [32].

TABLE IV. The LO (in brackets) and NLO total cross sections for $\eta_c + c + \bar{c}$, $\eta_b + b + \bar{b}$, $B_c + b + \bar{c}$ production via photon-photon fusion at $\sqrt{s} = 250$ GeV. Here the cut $1\ \text{GeV} \le p_t \le 50\ \text{GeV}$ is imposed.

Photon	$\sigma_{\eta_c c\bar{c}}$ (fb)	$\sigma_{\eta_b b\bar{b}}$ (fb)	$\sigma_{B_c b\bar{c}}$ (fb)
WWA	218.0(126.7)	0.068(0.055)	0.799(0.778)
LBS	1133(606)	3.67(2.08)	26.6(23.1)

Of the future high energy e^+e^- colliders, like the CEPC, the collision energy may reach 250 GeV [33]. And the LBS photon collision can be realized by imposing a laser beam to each e beam. Therefore, we investigate the $\eta_c + c + \bar{c}$, $\eta_b + b + \bar{b}$, and $B_c + b + \bar{c}$ productions under both WWA and LBS photon collisions with $\sqrt{s} = 250$ GeV. The corresponding LO and NLO total cross sections are presented in Table IV. As the energy scale of CEPC is higher than that of SuperKEKB, the K factors here are less than 2. Taking a typical luminosity $\mathcal{L} = 10^{34}\ \text{cm}^{-2}\,\text{s}^{-1}$ [23], the number of reconstructed $\eta_c + c + \bar{c}$ candidates per year is about 8.42×10^2 for the WWA photon case, 4.38×10^3 for the LBS photon case. For $\eta_b + b + \bar{b}$ production, the observation is somewhat difficult due to the insignificant production rates. For B_c inclusive production, it is not necessary to reconstruct the produced b and $\bar{c}$ jets. Assuming B_c is reconstructed through $B_c^{\pm} \to J/\psi(1S)\pi^{\pm}$, whose branching fraction is predicted

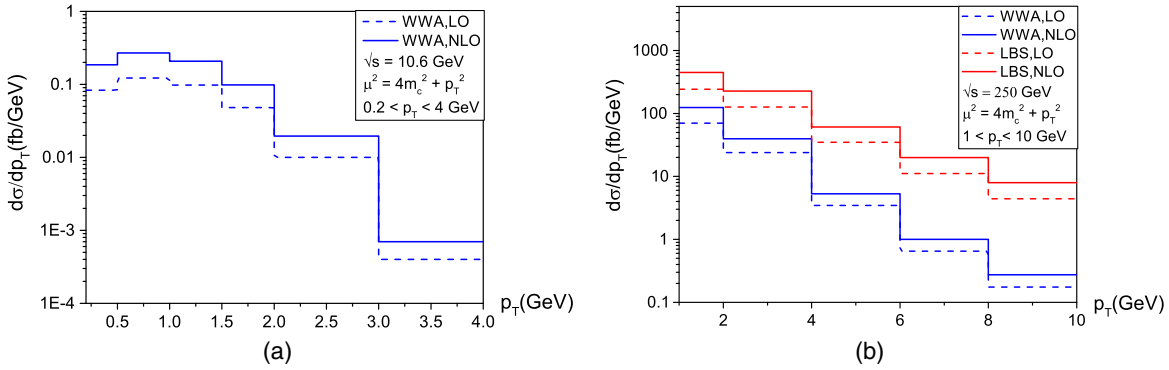

FIG. 4. The p_t distribution for the $\eta_c c\bar{c}$ production via photon-photon fusion at (a) the SuperKEKB collider and (b) the CEPC. Here the renormalization scale $\mu = \sqrt{4m_c^2 + p_t^2}$, the transverse momentum cut $0.2 \le p_t \le 4$ GeV and $1 \le p_t \le 10$ GeV is imposed on η_c, respectively.

to be 0.5% [34], and J/ψ is reconstructed through $J/\psi \to l^+l^-(l = e, \mu)$ with a branching fraction of about 12% [23], the number of the reconstructed B_c candidates for the LBS photon case would reach 10 per year. Note that, since B_c^* almost always decays to B_c, a more exact prediction on B_c candidates should take into account the $\gamma + \gamma \to B_c^* + b + \bar{c}$ process, and we leave it for future study.

As the number of events corresponding to $\eta_c + c + \bar{c}$ production is large, it is worthy to perform a more elaborate phenomenological analysis. The differential cross sections versus p_t, i.e., the transverse momentum of η_c, at the SuperKEKB collider and CEPC are shown in Fig. 4, the p_t at the CEPC is limited within 10 GeV due to the total cross section decreases rapidly versus p_t. It can be seen that the NLO corrections cause an upward shift of the LO distributions and leave the shapes nearly unchanged.

V. SUMMARY AND CONCLUSIONS

In this work, we investigate the $\eta_c + c + \bar{c}$, $\eta_b + b + \bar{b}$, $B_c + b + \bar{c}$ production via photon-photon fusion at the NLO QCD accuracy in the framework of NRQCD factorization formalism. The total cross sections and the differential cross sections versus transverse momentum at the SuperKEKB collider and the CEPC are given.

Numerical results shows that, after including the NLO corrections, the total cross sections are significantly enhanced, and their dependences on the renormalization scale and heavy quark mass parameter are reduced as expected. Due to the high luminosity of the SuperKEKB collider, the $\eta_c + c + \bar{c}$ production via photon-photon fusion is hopeful to be observed in the near future. At the higher energy collider like CEPC, the production rate of $\eta_c + c + \bar{c}$ is largely enhanced, which leads to inspiring events number. If the LBS photon collision can be realized, then the observation of B_c meson production at the CEPC can also be expected.

ACKNOWLEDGMENTS

This work was supported in part by the National Key Research and Development Program of China under Contract No. 2020YFA0406400, and the National Natural Science Foundation of China (NSFC) under Grants No. 11975236, No. 11635009, and No. 12047553.

[1] G. T. Bodwin, E. Braaten, and G. Lepage, Phys. Rev. D **51**, 1125 (1995); **55**, 5853(E) (1997).
[2] J. M. Campbell, F. Maltoni, and F. Tramontano, Phys. Rev. Lett. **98**, 252002 (2007).
[3] B. Gong and J. X. Wang, Phys. Rev. Lett. **100**, 232001 (2008).
[4] Y. Q. Ma, K. Wang, and K. T. Chao, Phys. Rev. Lett. **106**, 042002 (2011).
[5] M. Butenschoen and B. A. Kniehl, Phys. Rev. Lett. **106**, 022003 (2011).
[6] M. Klasen, B. A. Kniehl, L. Mihaila, and M. Steinhauser, Phys. Rev. Lett. **89**, 032001 (2002).
[7] C. F. Qiao and J. X. Wang, Phys. Rev. D **69**, 014015 (2004).
[8] R. Li and K. T. Chao, Phys. Rev. D **79**, 114020 (2009).
[9] Z. Sun, X. G. Wu, and H. F. Zhang, Phys. Rev. D **92**, 074021 (2015).
[10] P. Artoisenet, J. P. Lansberg, and F. Maltoni, Phys. Lett. B **653**, 60 (2007).
[11] C. H. Chang and Y. Q. Chen, Phys. Rev. D **48**, 4086 (1993).
[12] C. H. Chang, Y. Q. Chen, G. P. Han, and H. T. Jiang, Phys. Lett. B **364**, 78 (1995).
[13] A. V. Berezhnoy, A. K. Likhoded, and M. V. Shevlyagin, Phys. Lett. B **342**, 351 (1995).
[14] K. Kolodziej, A. Leike, and R. Ruckl, Phys. Lett. B **348**, 219 (1995).
[15] Z. Q. Chen, L. B. Chen, and C. F. Qiao, Phys. Rev. D **95**, 036001 (2017).
[16] S. Frixione, M. L. Mangano, P. Nason, and G. Ridolfi, Phys. Lett. B **319**, 339 (1993).
[17] I. Ginzburg, G. Kotkin, V. Serbo, and V. I. Telnov, Nucl. Instrum. Methods Phys. Res. **205**, 47 (1983).
[18] V. I. Telnov, Nucl. Instrum. Methods Phys. Res., Sect. A **294**, 72 (1990).
[19] G. T. Bodwin and A. Petrelli, Phys. Rev. D **66**, 094011 (2002); **87**, 039902(E) (2013).
[20] M. Krämer, Nucl. Phys. **B459**, 3 (1996).
[21] S. Dittmaier, Nucl. Phys. **B565**, 69 (2000).
[22] E. J. Eichten and C. Quigg, Phys. Rev. D **49**, 5845 (1994).
[23] P. A. Zyla *et al.* (Particle Data Group), Prog. Theor. Exp. Phys. **2020**, 083C01 (2020).
[24] B. Gong, L. P. Wan, J. X. Wang, and H. F. Zhang, Phys. Rev. Lett. **112**, 032001 (2014).
[25] X. C. Zheng, X. G. Wu, and X. D. Huang, J. High Energy Phys. 07 (2021) 014.
[26] M. Klasen, B. A. Kniehl, L. N. Mihaila, and M. Steinhauser, Nucl. Phys. **B713**, 487 (2005).
[27] Y. J. Zhang, Y. j. Gao, and K. T. Chao, Phys. Rev. Lett. **96**, 092001 (2006).
[28] Y. J. Zhang and K. T. Chao, Phys. Rev. Lett. **98**, 092003 (2007).

[29] http://www-superkekb.kek.jp/.
[30] M. Aaboud *et al.* (ATLAS Collaboration), Phys. Rev. Lett. **120**, 211802 (2018).
[31] P. Faccioli, V. Knünz, C. Lourenco, J. Seixas, and H. K. Wöhri, Phys. Lett. B **736**, 98 (2014).
[32] Z. B. Kang, Y. Q. Ma, J. W. Qiu, and G. Sterman, Phys. Rev. D **90**, 034006 (2014).
[33] J. B. Guimares da Costa *et al.* (CEPC Study Group), arXiv:1811.10545.
[34] C. H. Chang and Y. Q. Chen, Phys. Rev. D **49**, 3399 (1994).